Internalization study of nanosized zeolite crystals in human glioblastoma cells

C Hélaine, Hayriye Özçelik, Sarah Komaty, Abdallah Amedlous, Sajjad Ghojavand, Didier Goux, Richard Retoux, Svetlana Mintova, Valable Samuel

▶ **To cite this version:**

C Hélaine, Hayriye Özçelik, Sarah Komaty, Abdallah Amedlous, Sajjad Ghojavand, et al.. Internalization study of nanosized zeolite crystals in human glioblastoma cells. Colloids and Surfaces B: Biointerfaces, 2022, 218, pp.112732. 10.1016/j.colsurfb.2022.112732 . hal-03752239

HAL Id: hal-03752239
https://hal.science/hal-03752239v1

Submitted on 29 Aug 2022

HAL is a multi-disciplinary open access archive for the deposit and dissemination of scientific research documents, whether they are published or not. The documents may come from teaching and research institutions in France or abroad, or from public or private research centers.

L'archive ouverte pluridisciplinaire **HAL**, est destinée au dépôt et à la diffusion de documents scientifiques de niveau recherche, publiés ou non, émanant des établissements d'enseignement et de recherche français ou étrangers, des laboratoires publics ou privés.

Colloids and Surface B: Biointerfaces

Internalization Study of Nanosized Zeolite Crystals in Human Glioblastoma Cells

Charly Helaine[1], Hayriye Özçelik[1], Sarah Komaty[2], Abdallah Amedlous[2], Sajjad Ghojavand[2], Didier Goux[3, 4], Richard Retoux[4], Svetlana Mintova[2], Samuel Valable [1*]

[1]*Normandie Univ., UNICAEN, CNRS, ISTCT, GIP CYCERON, 14000 Caen, France.*

[2]*Normandie Univ., UNICAEN, CNRS, ENSICAEN, Laboratoire Catalyse et Spectrochimie, 14000 Caen, France.*

[3]*Normandie Univ., UNICAEN, CMAbio3, US EMerode, 14000 Caen, France.*

[4]*Normandie Univ., UNICAEN, CNRS, ENSICAEN, Laboratoire CRISMAT, 14000 Caen, France.*

** Correspondence: Dr Samuel Valable, ISTCT UMR6030; GIP CYCERON, Bd H Becquerel, BP5229, 14074 Caen Cedex, 33 2 31 47 01 08; samuel.valable@cnrs.fr*

Stastistical summary:

Words: 5,983

Figures: 5

ABSTRACT

While the use of nanozeolites for cancer treatment holds a great promise, it also requires a better understanding of the interaction between the zeolite nanoparticles and cancer cells and notably their internalization and biodistribution. It is particularly important in situation of hypoxia, a very common situations in aggressive cancers, which may change the energetic processes required for cellular uptake. Herein, we studied, *in vitro*, the kinetics of the internalization process and the intracellular localization of nanosized zeolite X (FAU-X) into glioblastoma cells. In normoxic conditions, scanning electron microscopy (SEM) showed a rapid cell membrane adhesion of zeolite nanoparticles (< 5 min following application in the cell medium), occurring before an energy-dependent uptake which appeared between 1 h and 4 h. Additionally, transmission electron microscopy (TEM) and flow cytometry analyzes, confirmed that the zeolite nanoparticles accumulate over time into the cytoplasm and were mostly located into vesicles visible at least up to 6 days. Interestingly, the uptake of zeolite nanoparticles was found to be dependent on oxygen concentration, *i.e.* an increase in internalization in severe hypoxia (0.2% of O_2) was observed. No toxicity of zeolite FAU-X nanoparticles was detected after 24 h and 72 h. The results clearly showed that the nanosized zeolites crystals were rapidly internalized *via* energy-requiring mechanism by cancer cells and even more in the hypoxic conditions. Once the zeolite nanoparticles were internalized into cells, they appeared to be safe and stable and therefore, they are envisioned to be used as carrier of various compounds to target cancer cells.

Keywords

Nanosized zeolite, Faujasite, Colloidal suspension, Glioblastoma, Cell uptake, Cytotoxicity.

1. Introduction

Glioblastoma is the most common and aggressive primary brain tumor in adults [1]. Despite conventional treatments, including radiotherapy and chemotherapy along with surgery, the median survival of patients does not exceed 15 months [2]. Because glioblastoma are characterized by a pronounced hypoxia associated to tortuous and permeable blood vessels at the origin of the enhanced permeability and retention (EPR) effect, a wide range of nanoparticles (NPs) like nanoscale porous materials provide opportunities to be explored as anti-cancer drugs carriers and/or gases delivery platform [3–6].

Among these nanoparticles, nanosized zeolites have recently attracted significant interest due to the prominent physicochemical features including variable structures, high surface areas, ion exchange ability, and chemical/colloidal stability under physiological conditions [7–9]. Particular attention has been given to nanosized faujasite type zeolite (FAU), which was considered as a promising candidate for biomedical applications and notably in glioblastoma context [5,10] due to the good biocompatibility, non-toxicity and high stability. We have previously reported the synthesis of organic template-free nanosized FAU with high crystallinity and a size in the range of 10-100 nm with a narrow particle size distribution and excellent colloidal stability [11]. The nanosized FAU was prepared in different cationic forms (Fe^{3+}, Cu^{2+}, Gd^{3+}) and used as drug and gas carrier that enabled tracking with MRI [5,12]. Indeed, after intravenous administration in rat bearing glioblastoma cells, the Gd loaded zeolites were found with MRI in the tumor bulk [5]. More recently, *in vitro* study with glioblastoma cells using nanozeolites with luminescent properties demonstrated their intracellular incorporation [13]. However, the internalization process of zeolites into glioblastoma cells and their precise intracellular localization is not clearly understood and require further studies. Some reports suggested that the NPs uptake is dependent

on various parameters such as size and charge but also is cell type-dependent [14–16]. As mentioned previously, it is also of great importance to consider the internalization of zeolite nanoparticles in hypoxic environment found in glioblastoma [17] in order to improve the NP-based cancer therapies. Only few studies have taken the hypoxic conditions into considerations [18,19] which however change energetic processes in cells [20].

Depending on various features of NPs (size, surface charge, composition), they can be internalized in cells by passive translocation or by an energy-requiring process called endocytosis [16]. Endocytosis can be categorized into (i) a phagocytosis which refers to special cells and allows to internalizes particles larger than 0.5 μm and aggregates, and (ii) a pinocytosis, a major way of internalization of small particles in eukaryotic cells [16]. According to the proteins involved, the pinocytosis is classified to macropinocytosis, clathrin-dependent endocytosis, caveolae-dependent endocytosis and clathrin-/caveolae-independent endocytosis [21]. Understanding the process of internalization of NPs and notably the subcellular localization may help to further tune their properties for biomedical use. For instance, if the Gd^{3+} doped NPs have to be used to improve the efficacy of radiotherapy based on the presence of heavy metal ion, *i.e.* Gd^{3+}, used as a radiosensitizer, and thanks to the restricted path of electrons in the cells after irradiation, a very close localization to the nucleus is required.

Herein, we investigated, *in vitro*, the kinetics of the internalization process and the intracellular localization of zeolite (Na-FAU-X) nanoparticles doped with Gd^{3+} (Gd-FAU-X) in U251-MG glioblastoma cells using scanning electron microscopy (SEM), transmission electron microscopy (TEM) and flow cytometry. Our results showed a rapid cell membrane adhesion (<5 min) of Gd-FAU-X followed by an intracellular uptake, mostly in vesicles. More interestingly, severe hypoxia (0.2% O_2), found in glioblastoma, increased the NPs uptake in the U251-MG cells

while moderate hypoxia did not. This study is of great importance since understand the uptake of zeolite nanoparticles by glioblastoma cells will allow their future use in biomedical applications.

2. Experimental section

2.1. Materials and chemicals

The following initial reagents were used for the preparation of the nanosized zeolites: Al powder (Al, 325 mesh, 99.5%, Alfa Aesar, Karlsruhe, Germany); sodium hydroxide (NaOH, 98%, Sigma-Aldrich, Saint-Quentin Fallavier, France); colloidal silica (SiO_2, Ludox-HS 30, 30 wt.% SiO_2, pH: 9.8, Sigma-Aldrich); Gadolinium(III) nitrate hexahydrate ($Gd(NO_3)_3$, $6H_20$, 99.99%, Sigma-Aldrich); ruthenium chloride (99.9%, (PGM basis); Ru 38% min, Alfa Aesar, Karlsruhe, Germany); 2,2'-dipyridyl (99+ %, Acros Organics, Geel, Belgium); N,N-dimethylformamide (DMF, 99.8+ %, Alfa Aesar); lithium chloride (99+ %, Thermo Fisher Scientific, Geel, Belgium); acetonitrile anhydrous (99.9+ %, Extra Dry, AcroSeal®, ACROS Organics); absolute ethanol (≥99.5%, Sigma-Aldrich); and diethyl ether (99+ %, ACROS Organics).

The following initial reagents were used for the biological characterization: two human glioblastoma-derived cell lines, U251-MG cells (Cellosaurus CVCL_0021) purchased from National Cancer Institute (NCI, Bethesda, MD, USA) and U87-MG cells (Cellosaurus CVCL_0022) obtained from the American Type Culture Collection (ATCC, LGC standards, Molsheim, France). All chemical products used for biological characterization were purchased from Sigma-Aldrich, exceptions were notified in the text.

2.2. Synthesis of nanosized zeolites

Nanosized faujasite-X (Na-FAU-X) zeolite with Si/Al ratio of 1.3 and particle size below 25 nm was synthetized from a clear colloidal precursor suspension as described previously [11]. The formed crystals were stabilized in water suspension with a concentration of 2.5 wt.%.

The as-synthesized nanosized Na-FAU-X zeolite was subjected to Gd-exchange at room temperature. The Gd-exchange sample was prepared using 5 mL of Na-FAU-X zeolite suspension with the concentration of 2.5 wt.% mixed with 25 mL of Gd $(NO_3)_3 \cdot 6H_2O$ (3 mM); the mixture was kept under stirring at room temperature for 1 h and then the sample was washed by double distilled water (ddH_2O); this procedure was repeated twice and the final suspension was purified with ddH_2O using high speed centrifugation (20000 rpm for 30 min) and the sample was re-dispersed in double distilled water (Gd-FAU-X).

The nanosized FAU zeolite containing ruthenium complex ($Ru(bpy)_3$-FAU) was used as a solid and as a colloidal suspension in double distilled water; the $Ru(bpy)_3$-FAU was prepared according to the method reported by our group [13].

2.3. Characterization

X-ray powder diffraction (XRD) analysis: XRD patterns were collected using a PANalytical X'Pert Pro diffractometer with CuKα monochromatized radiation (λ = 1.5418 Å). The samples were scanned in the range of 4–50 °2θ with a step size of 0.02°.

Dynamic light scattering (DLS) and zeta potential analysis: The size of zeolite particles was determined by a Malvern Zetasizer Nano DLS instrument using a backscattering geometry (scattering angle of 173°, He-Ne laser with a 3 mW output power at a wavelength of 632.8 nm).

This analysis was performed using a zeolite suspension of 1 wt.% in ddH_2O. The surface charge of the nanosized zeolite crystals was measured by conducting zeta potential measurements of the same suspension pH= 7.

Inductively coupled plasma mass spectrometry (ICP-MS): The chemical composition of the zeolite samples was characterized by inductively coupled plasma (ICP) optical emission spectroscopy using a Varian ICP-OES 720-ES. The samples for the ICP were prepared according to the following procedure: (i) 50 mg of sample was dissolved in 3 mL of hydrofluoric acid (HF) (40−45%), then (ii) a 0.5 mL of mixture (HNO_3/HCl ≡ 1:3 v/v) was added and heated at 110 °C for 1 h in the polytetrafluoroethylene (PTFE) bottle (100 mL), and (iii) 96.5 mL of double distillated water and 2 g of boric acid (H_3BO_3) were added. The resulting solution was stirred overnight to facilitate dissolution of the boric acid. Finally, 10 mL of the solution was diluted 10 times with double distillated water before analysis.

N_2 sorption analysis: N_2 adsorption/desorption isotherms of zeolite powder samples were measured by a Micrometrics ASAP 2020 volumetric adsorption analyzer. Samples were degassed at 250 °C under vacuum overnight before the measurements. The external surface area and micropore volume were assessed by alpha-plot method using Silica-1000 (22.1 m^2/g assumed) as a reference. The micropore and mesopore size distributions of solids were extracted from the adsorption branch using the Nonlocal Density Functional Theory (NLDFT) method and from the desorption branch using the Barret-Joyner-Halenda (BJH) algorithm, respectively.

Thermogravimetric (TGA) analysis: The thermal behavior of the zeolite powder samples was investigated by TGA using a SETSYS instrument (SETARAM) analyzer in the temperature range 25 - 800 °C with a heating rate of 10 °C/min under air with a flow of 40 mL/min.

2.4. Biological characterization of nanosized zeolites

Cell culture: The human glioblastoma-derived cell line U251-MG and U87-MG were cultured in DMEM 1 g/l of glucose supplemented with 10% fetal calf serum, 2 mM L-glutamine, 100 U/mL penicillin and 100 µg/mL streptomycin. The cell line was maintained in culture at 37°C with 5% CO_2 and 95% humidity. Cells were seeded at $2.5.10^4$ cells/mL but for experiments lasting 144 h, the cell seeding density was 1.10^4 cells/mL.

Hypoxia: Hypoxia experiments were performed in a hypoxia workstation (IN VIVO 2 500, Baker Ruskinn, Alliance Bio Expertise, Guipry, France) set at 1% or 0.2% O_2, 5% CO_2 at 37 °C in humidified atmosphere. Culture medium was equilibrated at least 30 min with the gas mixture before being added to the cells and incubated in the hypoxia chamber. U251-MG and U87-MG cells were maintained under hypoxic (1 or 0.2% O_2) or normoxic (21% O_2) conditions until the end of experiments (4 h or 24 h).

Flow cytometry analyses: The cell uptake of $Ru(bpy)_3$-FAU-X nanosized zeolite into U251-MG cells was investigated using a flow cytometry. The luminescent zeolite crystals were studied for 4 h at 4°C or 37 °C and for 24 h at 37 °C, living cells were washed and immediately analyzed using the CytoFLEX S flow cytometer (Beckman Coulter SAS, US PLATON, Caen, France). Briefly, the living single cell population was gated after excluding doublets, cell debris and zeolites nanoparticles in suspension and a histogram from the Violet-610 channel was analyzed using the CytExpert Flow Analysis Software (Beckman Coulter SAS, Villepinte, France).

Transmission electron microscopy (TEM): Cells were fixed with 2.5% glutaraldehyde in 0.1 M sodium cacodylate buffer pH 7.4, rinsed in the same buffer and then post-fixed with 1% osmium tetroxide in sodium cacodylate buffer for 1 h at RT under dark conditions. Then the samples were

rinsed, dehydrated by ethanol treatment (70%, 95%, 100%) and subsequently embedded in progressive concentration of Embed 812 resin using absolute ethanol (50%, 75%, 100%) and polymerized at 60 °C for 48 h. Ultrathin sections (80 nm) of cells were prepared using a Leica Ultracut R ultramicrotome and deposited on 200-mesh copper grids. Sections were stained with an aqueous solution of 5% uranyl acetate for 30 min, followed by Reynold's lead citrate staining for 5 min. Then the stained cells sections were investigated using JEOL 1011 and JEOL F200 Transmission Electron Microscope equipped with energy dispersive X-ray (EDX) detector, both operating at 80 kV for taking images and analysing the chemical composition, respectively.

Scanning electron microscopy (SEM): Cells were fixed with 2.5% glutaraldehyde in 0.1 M sodium cacodylate buffer (pH 7.4) and then dehydrated by using ethanol (70%, 95%, 100%) and critical point drying (CPD 030 LEICA Microsystem). Then the samples were coated with platinum and characterized by a ZEISS SUPRA 55 Scanning Electron Microscope at 3kV equipped with a BRUKER X-flash 6160 EDX detector.

Cell viability: Cell viability analyses were performed after exposure to nanosized zeolites for 24 h and 72 h with a WST-1 assay (Roche, Bale, Switzerland) according to the manufacturer's instruction.

Statistical analysis: Statistical analyses were performed with Statistica® (Tibco Software Inc, Palo Alto, CA, USA). Data are presented as mean value± standard deviation (SD); the tests and the number of experiments used are detailed in each figure legend.

3. Results and Discussion

3.1. Characterization of nanosized FAU-based zeolites

The main physicochemical properties of nanosized Na-FAU-X, Gd-FAU-X and $Ru(bpy)_3$-FAU-X zeolite samples are presented in the supporting information. All samples exhibited the diffraction peaks typical for FAU type framework (**Figure S1**). The size and morphology of the crystals characterized by SEM are shown in **Figure S2**. In addition, the hydrodynamic diameter of the nanosized crystals was followed by DLS. The DLS curves for both samples show a narrow, monomodal particle size distribution with a hydrodynamic diameter between 15 and 40 nm (**Figure S3**). The zeta potential for Na-FAU-X and Gd-FAU-X colloidal suspensions was -38 and -43 mV, respectively, which indicates their high colloidal stability (**Figure S4**). The elemental composition of the Na-FAU-X and Gd-FAU-X samples using ICP-MS are summarized in **Table S1**. No significant changes in the Si/Al ratio of the samples was measured, both samples have a Si/Al of 1.3. The amount of Gd^{3+} loaded in the Gd-FAU-X sample was found to be 1.94 wt.%. Both samples exhibit two decomposition stages in the TG curves (**Figure S5**), corresponding to water adsorbed on the surface and in the channels of the nanosized zeolite. The total amount of water for Na-FAU-X and Gd-FAU-X samples was 45 and 35%, respectively. The textural properties of samples were measured by nitrogen adsorption and the results are summarized in **Table S2**. The nitrogen adsorption isotherms of samples Na-FAU-X and Gd-FAU-X are shown in **Figure S6**. Both isotherms show a type I and type IV isotherms, typical of microporous materials with textural mesoporosity due to the close packing of nanocrystals with similar size and morphology. The samples exhibit high external surface area of 785 and 685 m^2/g for Na-FAU-X and Gd-FAU-X, respectively. The characterization of sample $Ru(bpy)_3$-FAU-X can be found in our recent article [13].

3.2. Kinetic study of zeolite adhesion on the U251-MG cell membrane

In order to exploit the potential of nanosized Gd-FAU-X zeolite for biomedical application, it is important to further understand the tight interactions of NP with the cells. For this purpose, SEM experiments were performed on U251-MG cells incubated with 100 µg/mL of Gd-FAU-X zeolites for 5 and 60 min in the cell medium (**Figure 1A**). SEM results showed that Gd-FAU-X zeolite nanocrystals as cluster were found attached to the cell membrane after 5 min of incubation (**Figure 1A, arrow**). Upon increasing the incubation time to 60 min, the particles were still present on cell membrane and interestingly accumulated on its surface (**Figure 1A**). To further confirm that the Gd-FAU-X zeolites were present in the U251-MG cells (**Figure 1B**), SEM/EDX analysis after 60 min of incubation with 100 µg/mL Gd-FAU-X nanocrystals were performed and compared with a zeolite-free area of the cells named control zone (**Figure 1B**). The results displayed an increase in the energy peaks corresponding to the characteristic zeolite elements like oxygen (O), sodium (Na), aluminum (Al) and silica (Si) in comparison to the control zone whereas the energy peak of carbon (C) employed as a negative control decreased. Element mapping analysis of U251-MG cells incubated with 100 µg/mL of Gd-FAU-X zeolites after 60 min using SEM/EDX is depicted in **Figure 1C**. The results show a colocalization for Na, Al and O elements with the presence of zeolites clusters using TEM bright field image, while the C appeared with less intensity (**Figure 1C**). These results suggest that Gd-FAU-X zeolite crystals are able to rapidly attach to the cell membrane after addition in the cell medium. Indeed, these NPs are small (<50 nm), that facilitate uptake and interactions with cell membrane, as described by Lu *et al* [22]. The Gd-FAU-X are negatively charged NPs and it has been shown that the uptake of negatively NPs is cell-type-dependent [16]. Here, the rapid attachment of the NPs to the membrane can be considered as the first step of internalization.

A

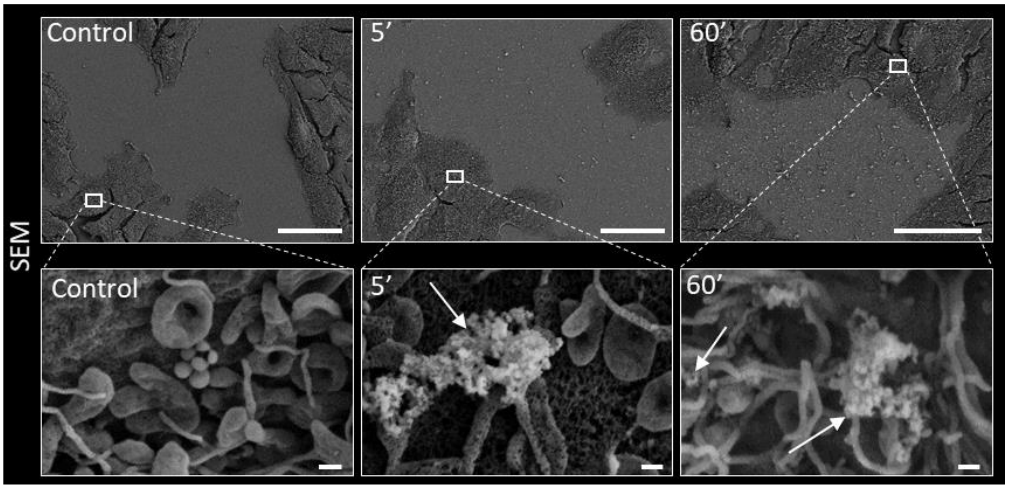
SEM
Control
5′
60′
Control
5′
60′

B

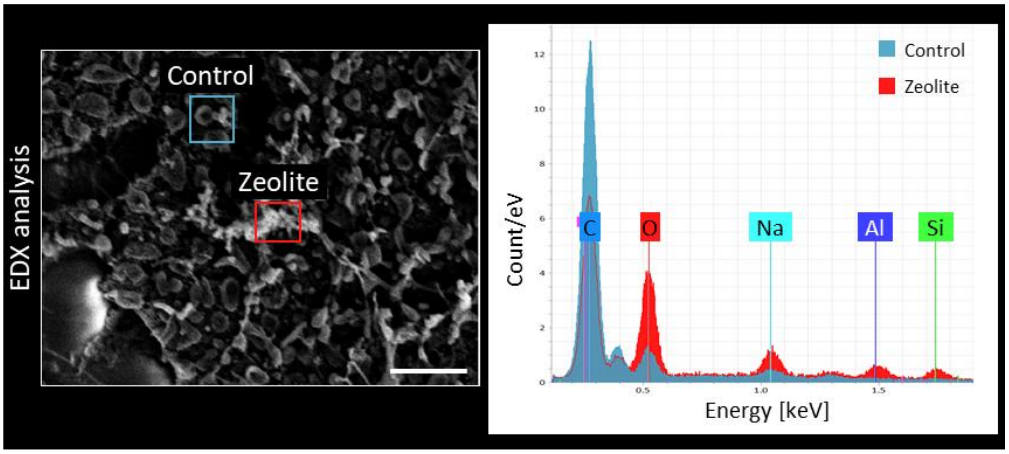
EDX analysis
Control
Zeolite
Control
Zeolite
Count/eV
C
O
Na
Al
Si
Energy [keV]

C

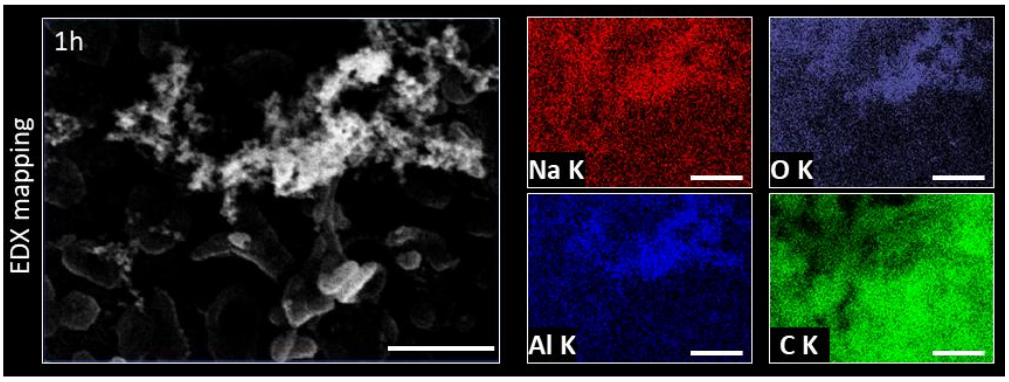
EDX mapping
1h
Na K
O K
Al K
C K

Figure 1. (A) Representative SEM micrographs of U251-MG cells after 5 min and 60 min exposure to 100 µg/mL of Gd-FAU-X zeolites and a control sample without zeolite. Scale bars: (top) 50 µm and (bottom) 200 nm. (B) SEM micrograph and the corresponding EDX spectra. The absorption peaks correspond to carbon (C), oxygen (O), sodium (Na), aluminum (Al) and silicon (Si). The blue and red squares correspond to the control and zeolite zones respectively. Scale bar: 2 µm. (C) SEM micrograph and the EDX mapping for sodium (Na K), aluminum (Al K), oxygen (O K) and carbon (C K) in the scanned area. Carbon was employed as negative control since no C was present in the zeolite samples. Scale bars: 1 µm.

3.3. Kinetic study of zeolite uptake in U251-MG glioblastoma cells

The cell adhesion (interaction) of zeolite nanoparticles with the cell membrane was revealed by SEM. In order to confirm the internalization and localization of zeolite nanoparticles in the cells, TEM study was performed on samples after different incubation periods. The intracellular localization of nanosized Gd-FAU-X zeolite crystals in the U251-MG cells was determined after 1, 4, 24, 72 and 144 h of incubation using 100 µg/mL of nanosized zeolite. Results clearly showed an internalization of Gd-FAU-X nanocrystals inside the glioblastoma cells. At 1 h, the zeolite nanoparticles were found in the cell membrane suggesting that they were ingested by cancer cells (**Figure 2A/1 h**). This process evolves in time, the internalization of zeolites and the formation of zeolite-containing vesicles were observed after 4 h (**Figure 2A/4 h**). While after 24 h, the zeolite crystals were found inside the cells and more precisely within vesicles, each containing of several zeolite nanoparticles (**Figure 2A/24 h**). The vesicles accumulated in time and were still detected in the cells after 72 h and 144 h (**Figure 2A/72 h and 144 h**). Importantly, the vesicles got closer to nucleus membrane over time. For example, at 144 h, the closest vesicles to the nucleus membrane were at a distance of 320 nm while at 24 hours it was at 620 nm. This finding is of great

importance especially in the case when zeolites are considered to be used as a carrier of heavy atoms such as Gd, known to release photoelectrons or generate high destructive electrons. For example, it was reported that auger electrons after irradiation were able to browse distances less than 1 μm through tissue [23]. Moreover, at 72 h, the zeolites-containing vesicles were distributed uniformly over the U251-MG cells using a transverse view (**Figure S7**).

To further confirm that the vesicles contain nanosized zeolite crystals, we performed chemical mapping after 24 h of incubation with 100 μg/mL of Gd-FAU-X nanocrystals. All elements originating from the zeolite crystals (Na, Al, Si and O) were detected by EDS; the zeolite crystals are also observed in the TEM bright field image (**Figure 2B**).

The TEM results of U251-MG cell line showed that the zeolites were internalized by tumor cells, and localized mainly in the vesicles. Interestingly, the kinetics study revealed that the zeolite-containing vesicles were still found inside the cells till 6 days (144 h). The results suggested an absence of exocytosis of the nanozeolites, in line with previous reports. Indeed, using gold NP (Au NP) and nanoporous silica NP (SiO_2 NPs), a intracellular decrease with time was reported due to cell proliferation but not as a result of exocytosis [24]. However, a decrease in the amount of zeolite NPs in the cells with time was observed and attributed to the cell division; a similar trend was seen for Gd-FAU-X zeolite crystals in glioblastoma cells (**Figure S8**). These results could be of great interest for future application of nanozeolites as a delivery system, since after cell incorporation they do not seem to be secreted but rather transmitted to daughter cells. Besides, the integrity of the Gd-FAU-X nanocrystals inside the vesicles is preserved over the time, (**Figure 2A, Inset**) thanks to their high structural stability. Indeed, zeolite nanocrystals are very stable solids that resist various conditions in contrast to other materials.

A

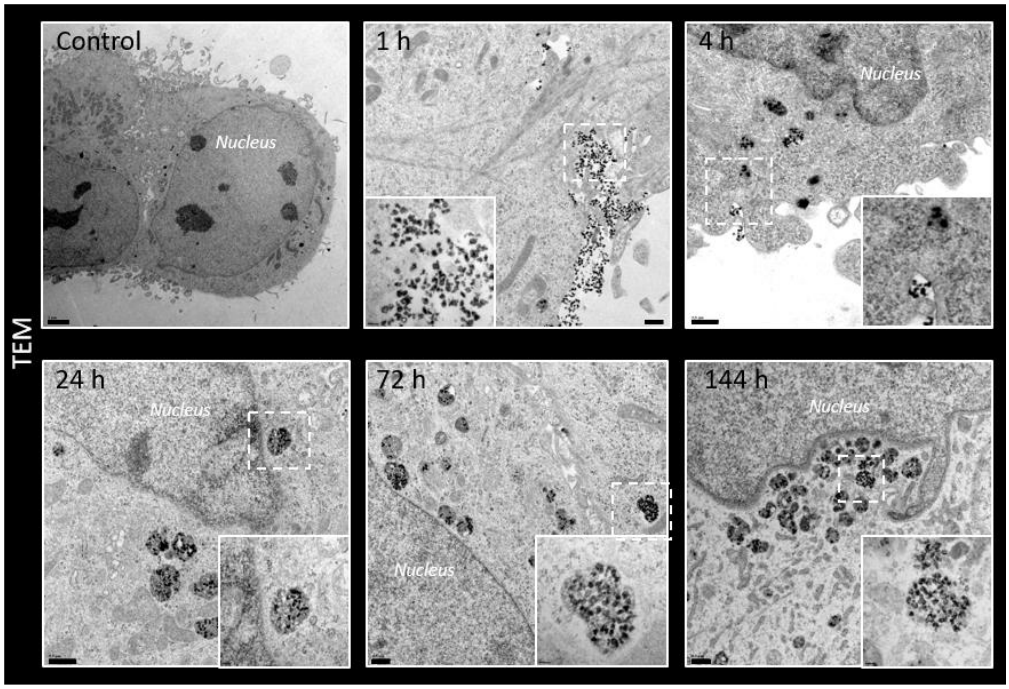
TEM
Control
Nucleus
1 h
4 h
Nucleus
24 h
Nucleus
72 h
Nucleus
144 h
Nucleus

B

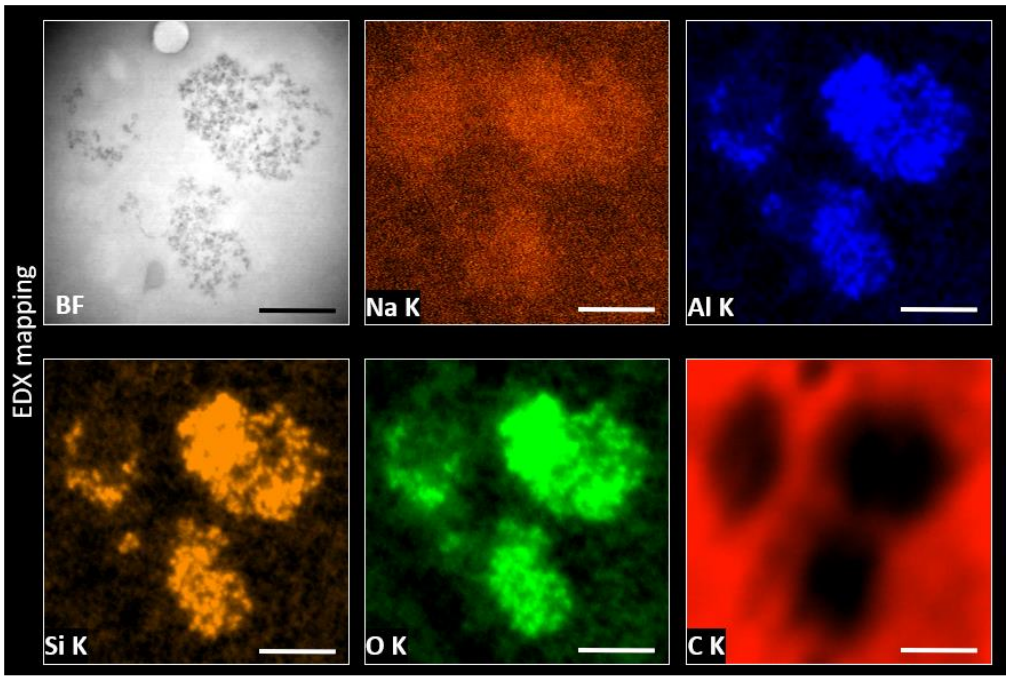
EDX mapping
BF
Na K
Al K
Si K
O K
C K

Figure 2. (A) Representative TEM micrographs of U251-MG cells after 1, 4, 24, 72 and 144 h exposure to 100 μg/mL of Gd-FAU-X zeolites and a control sample (without zeolite); Inset: magnified images of zeolite nanoparticles. Scale bars: 0.5 μm. (B) TEM bright field image and the corresponding EDX mapping for sodium (Na), aluminum (Al), silica (Si), oxygen (O) and carbon (C) in the same area. Carbon is employed as a negative control. Scale bars: 0.5 μm.

TEM study was performed on cells with nanosized Na-FAU-X zeolites and similar results were obtained (**Figure S9**) thus suggesting that internalization process may be comparable to the one reported for Gd-FAU-X.

In order to have a semi-quantitative analysis, flow cytometry analyses of cells containing luminescent zeolite nanocrystals were performed. Thus we used the $Ru(bpy)_3$-FAU zeolite-X, previously reported by our group [13]. Indeed, the incorporation of ruthenium-tris(2,2'-bipyridyl) ($Ru(bpy)_3$) complex in the FAU-X zeolite allowed to act as a luminescent probe detectable by flow cytometry [13]. We quantified the percentage of U251-MG cells containing $Ru(bpy)_3$-FAU-X 4 h zeolite nanocrystals with concentrations of 10 μg/mL and 100 μg/mL with different oxygen concentrations of 21%, 1% and 0.2% for 24 h (**Figure 3**). As shown in Figure 3A, B, C, the percentage of cells containing $Ru(bpy)_3$-FAU-X increased in a dose- and time-dependent manner. The results are in agreement with other studies demonstrating that the cellular internalization of NPs was time-dependent [15,25,26]. Moreover, an effect of oxygen concentration was found; more cells appeared to contain $Ru(bpy)_3$-FAU-X nanozeolites following treatment in severe hypoxia (0.2%) rather than mild hypoxia (1%) or normoxia, and these observations stands for the two concentrations used of 10 μg/mL and 100 μg/mL of $Ru(bpy)_3$-FAU-X nanocrystals (**Figure 3D,**

E). The current results are also in agreement with other studies reporting that uptake of AgNPs by U251-MG cells is higher under hypoxia rather than normoxia condition [18]. Surprisingly, we cannot observe this oxygen effect with another glioblastoma U87-MG cell line (**Figure S10**). In the aggressive brain tumors where severe hypoxia is found [17], the use of zeolite nanocrystals as nano-vector would be an attractive strategy particularly for hypoxic tumors treatment. Being able to target the most hypoxic cells would make them very appealing since these cells will be the most resistant cells after conventional treatments [27,28].

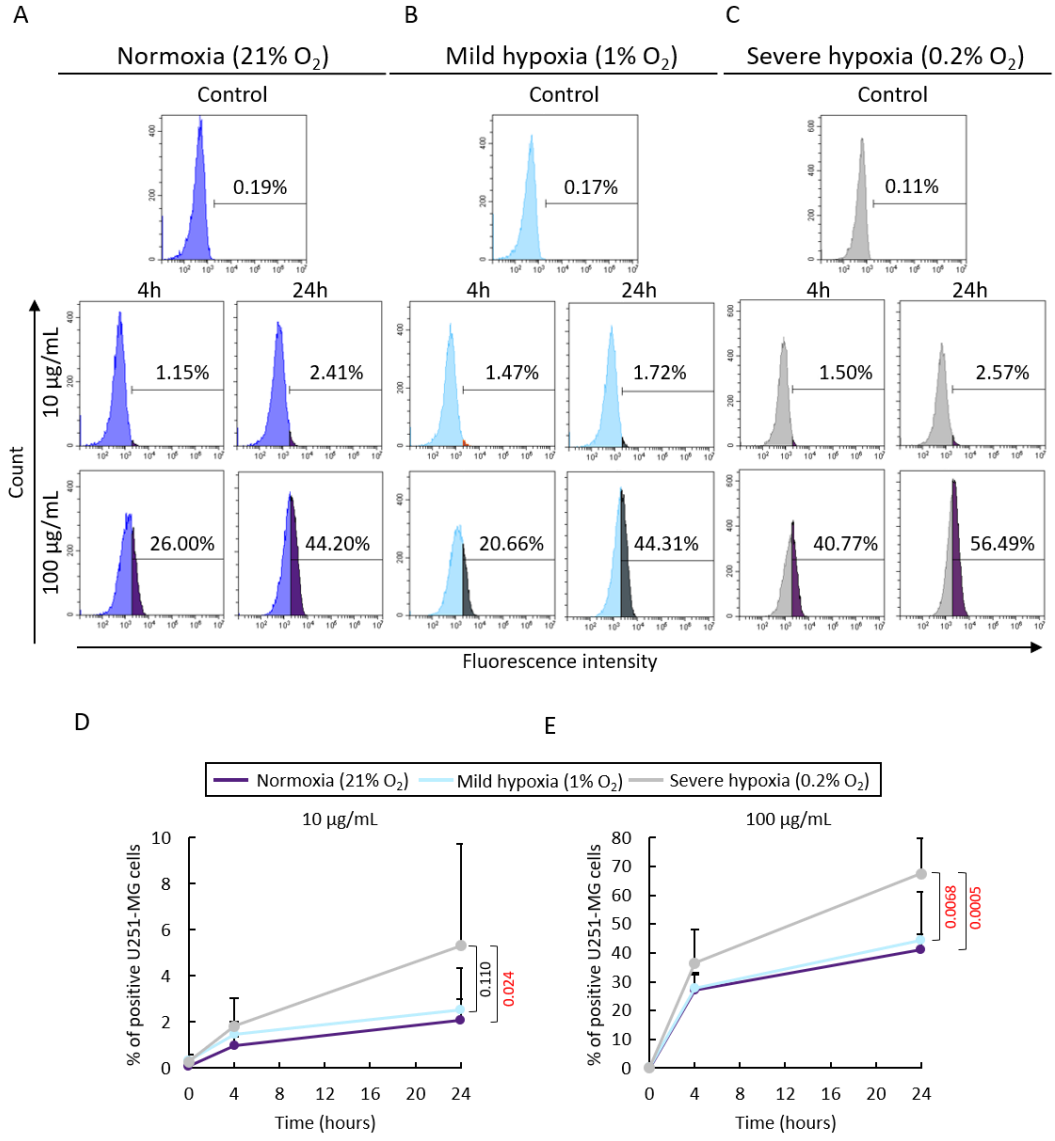

Figure 3. Representative histograms (A, B, C) of $Ru(bpy)_3$-FAU-X zeolite nanocrystals with increased concentrations (10 µg/mL, 100 µg/mL) in U251-MG cells after 4 h and 24 h and control cells (without zeolite) in normoxia (A), mild 1% hypoxia (B) and severe 0.2% hypoxia (C). Quantification (D, E, F) of cells containing $Ru(bpy)_3$-FAU-X zeolite nanocrystals after 4 h and 24 h incubation with 10 µg/mL (D) and 100 µg/mL (E) depending to oxygen level. Mean ± SD, N=3 ANOVA followed by Tukey's test.

In order to understand the internalization process of zeolite nanocrystals, we studied the $Ru(bpy)_3$-FAU-X uptake by U251-MG at lower temperature (4 °C) during 4 h, to disable energy-dependent processes by flow cytometry. A reduction of about 75% of the NPs internalization at 4 °C was found (**Figure 4**), allowing to conclude that zeolite internalization was based on an energetic process such as endocytosis [29]. This effect is well described in the literature for others particles but also including zeolites [26,30,31]. A close inspection of the U251-MG cells by TEM, revealed multiple Gd-FAU-X particles internalized by macropinocytosis with formation of membrane protrusions, called filopodia (or pseudopodia) after 1 h (**Figure 4C, black arrows**). The Gd-FAU-X particles in small invagination morphologically similar with clathrin- or caveolin-coated vesicles were detected after 4 h (**Figure 4C, white arrows**). The results clearly indicate that zeolite nanocrystals follow several endocytic pathways, as mentioned by Vilaça *et al*. [26].

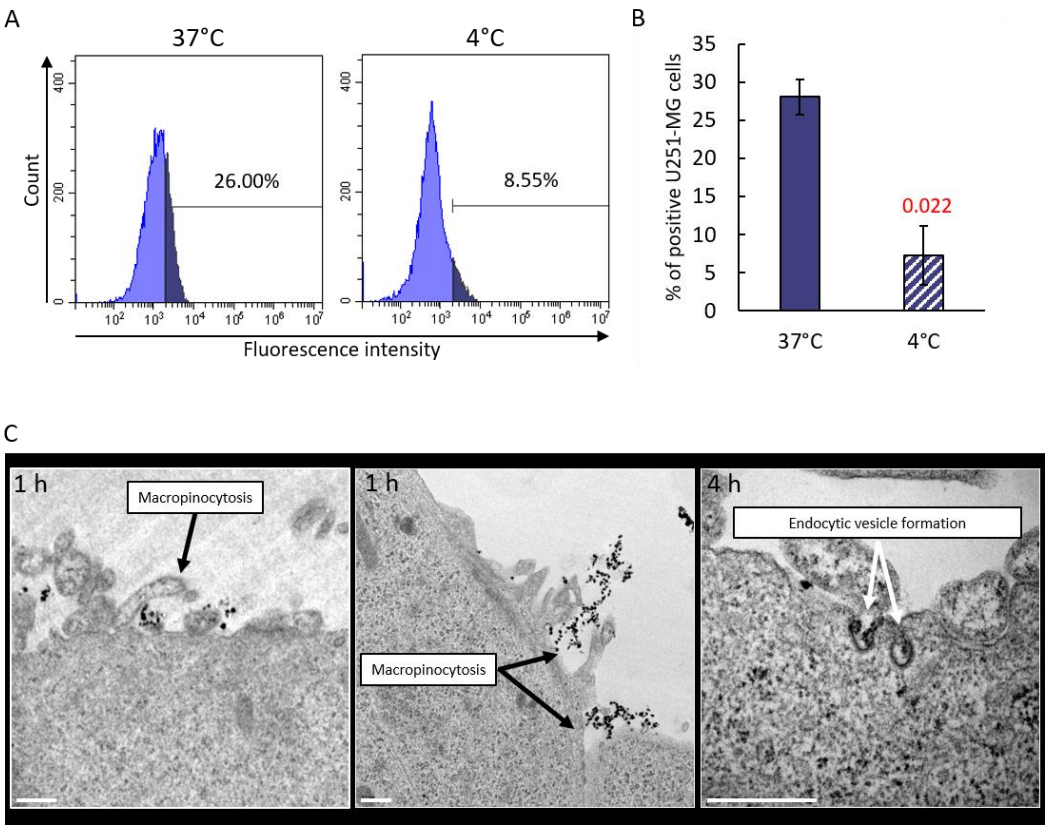

Figure 4. (A) Representative histograms of Ru(bpy)$_3$-FAU-X nanosized zeolite uptake in U251-MG cells after 4 h exposure to zeolites (100µg/mL) at 37 °C and 4 °C. (B) Quantification of cells containing Ru(bpy)$_3$-FAU-X zeolite crystals after 4 h incubation with 100 µg/mL at 37 °C and 4 °C. Mean ± SD, N=3, t-test. (C) Representative TEM micrographs of U251-MG cells after exposure to 100 µg/mL of Gd-FAU-X zeolites. Scale bars: 500 nm. Shown are electron micrographs illustrating the macropynocytosis (C, left and middle panels, black arrows) and the presence of zeolites nanocrystals in clathrin- or caveolin-coated vesicles (C, right panels, white arrows) in U251-MG cells.

3.4. Cytotoxicity study of nanosized zeolite nanoparticles on U251-MG glioblastoma cells

To assess the biocompatibility of nanozeolites in order to prove their applicability in biomedicine, cytotoxicity measurements were performed. U251-MG cells were exposed to zeolite nanocrystals at various concentrations (10 – 100 μg/mL) for 24 h and 72 h, followed by cell viability measurements. As shown in **Figure 5**, the U251-MG cell viability was not affected by exposure to both Na-FAU-X and Gd-FAU-X nanosized zeolites. We can conclude that the Gd-FAU-X zeolite nanocrystals are safe for these cells despite their presence inside the cells. These results are very interesting pointing out the possible biomedical application of nanozeolites as radiosensitizer or drug delivery system. It is also attested by the ability of cells to proliferate as showed in **Figure S8**.

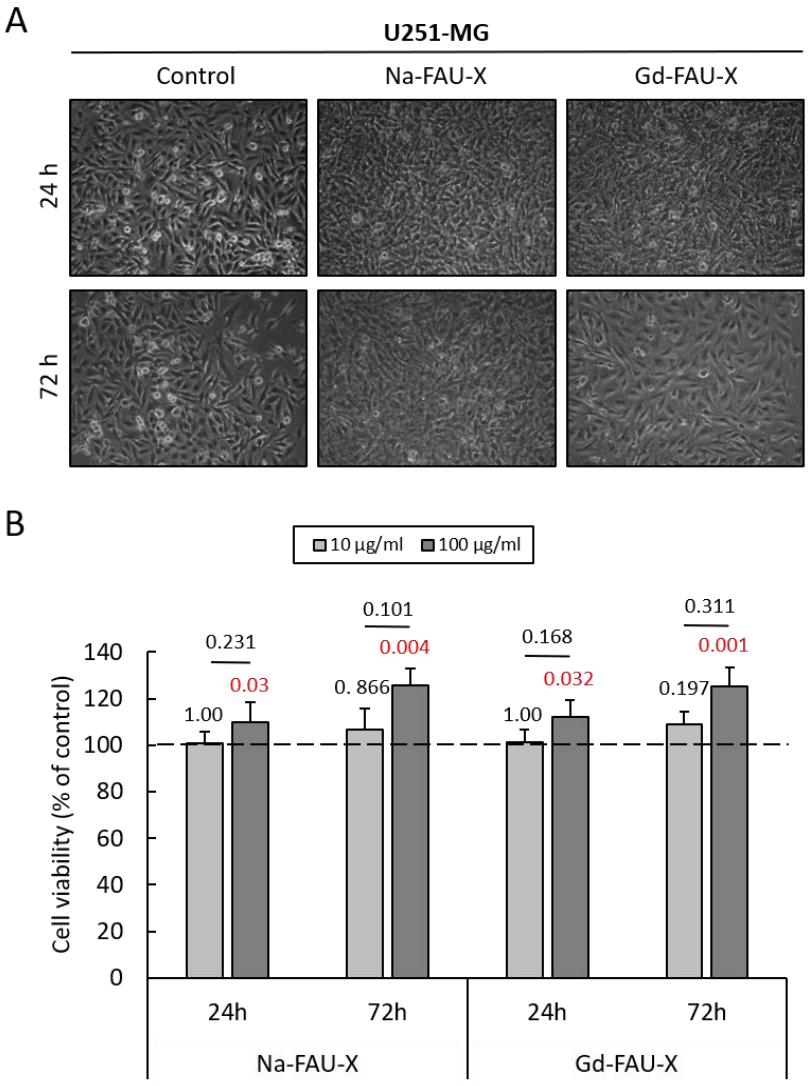

Figure 5. (A) Representative photographs in phase contrast of U251-MG cells after 24 h and 72 h exposure to 100 µg/mL of Na-FAU-X, Gd-FAU-X zeolite nanocrystals and a control (H_2O). (B) Quantification of U251-MG viability after 24 and 72 h exposed to various concentrations of Na-FAU-X and Gd-FAU-X zeolites. Cell viability was assessed using the WST-1 test. Mean ± SD, N=5, Kruskall-Wallis test.

4. Conclusions

In this work we report on the process of zeolites internalization by glioblastoma cells. The zeolites internalization begins quickly after zeolites exposure, and the particles are attached to the cell membrane after 5 min. Both the TEM and flow cytometry analyses pointed out an internalization of zeolites over time, and the zeolites-containing vesicles were mainly found. Interestingly, the internalization process was faster and greater in severe hypoxia without apparent exocytosis which further shed light the interest in zeolites, especially since the cell viability was not affected in U251-MG glioblastoma cells.

The internalization, stability and cytotoxicity results presented for the first time here reinforce the interest in nanosized zeolites as drug/gases delivery system for biomedical application and particularly in hypoxic tumors which are more radioresistant. Thanks to their increased surface area relative to micron-sized particles, nanocrystals offer a unique opportunity to carry high amount of drugs or other related compounds while limiting the need to inject high quantity not feasible for translational studies in patients. The smaller size of zeolite crystals also favors a higher intracellular uptake but also an intratumoral accumulation after intravenous administration.

As perspective, the localization of Gd-doped NPs closest to the nucleus, highlight the interest of this component as radiosensitizer, especially since in a previous work we demonstrated, *in vivo*, a specific accumulation of this Gd-FAU-X nanocrystal in the brain tumor after tail injection.

CREDIT AUTHORSHIP CONTRIBUTION STATEMENT

CH; HO performed all experiments on cells; SK; AA; SG conducted synthesis and physico-chemical characterizations; CH, DG and RR performed SEM, TEM and EDX analyses. SM and SV designed the study and interpreted the data. All authors drafted and edited the MS.

DECLARATION OF COMPETING INTEREST

Nothing to declare.

ACKNOWLEDGEMENT

The authors would like to thanks M. Xavier Larose Laboratoire CRISMAT (Normandie Univ, UNICAEN, CNRS, ENSICAEN, CRISMAT, 14000 Caen, France) for technical SEM support for microscopy observations.

FUNDING

The financial supports provided by Conseil Régional de Normandie, the European Union-Fonds Européen de Développement Régional (FEDER), Institut National du Cancer (INCA-11699) and

CNRS Innovation and Label of Excellence for the Centre for zeolites and nanoporous materials by the Region of Normandy (CLEAR) are acknowledged.

REFERENCES

[1] D.N. Louis, A. Perry, P. Wesseling, D.J. Brat, I.A. Cree, D. Figarella-Branger, C. Hawkins, H.K. Ng, S.M. Pfister, G. Reifenberger, R. Soffietti, A. von Deimling, D.W. Ellison, The 2021 WHO Classification of Tumors of the Central Nervous System: a summary, Neuro-Oncol. 23 (2021) 1231–1251. https://doi.org/10.1093/neuonc/noab106.

[2] P.Y. Wen, M. Weller, E.Q. Lee, B.M. Alexander, J.S. Barnholtz-Sloan, F.P. Barthel, T.T. Batchelor, R.S. Bindra, S.M. Chang, E.A. Chiocca, T.F. Cloughesy, J.F. DeGroot, E. Galanis, M.R. Gilbert, M.E. Hegi, C. Horbinski, R.Y. Huang, A.B. Lassman, E. Le Rhun, M. Lim, M.P. Mehta, I.K. Mellinghoff, G. Minniti, D. Nathanson, M. Platten, M. Preusser, P. Roth, M. Sanson, D. Schiff, S.C. Short, M.J.B. Taphoorn, J.-C. Tonn, J. Tsang, R.G.W. Verhaak, A. von Deimling, W. Wick, G. Zadeh, D.A. Reardon, K.D. Aldape, M.J. van den Bent, Glioblastoma in adults: a Society for Neuro-Oncology (SNO) and European Society of Neuro-Oncology (EANO) consensus review on current management and future directions, Neuro-Oncol. 22 (2020) 1073–1113. https://doi.org/10.1093/neuonc/noaa106.

[3] N. Martinho, C. Damgé, C.P. Reis, Recent Advances in Drug Delivery Systems, J. Biomater. Nanobiotechnology. 02 (2011) 510. https://doi.org/10.4236/jbnb.2011.225062.

[4] S.C. Baetke, T. Lammers, F. Kiessling, Applications of nanoparticles for diagnosis and therapy of cancer, Br. J. Radiol. 88 (2015) 20150207. https://doi.org/10.1259/bjr.20150207.

[5] C. Anfray, S. Komaty, A. Corroyer-Dulmont, M. Zaarour, C. Helaine, H. Ozcelik, C. Allioux, J. Toutain, K. Goldyn, E. Petit, K. Bordji, M. Bernaudin, V. Valtchev, O. Touzani, S. Mintova, S. Valable, Nanosized zeolites as a gas delivery platform in a glioblastoma model, Biomaterials. 257 (2020) 120249. https://doi.org/10.1016/j.biomaterials.2020.120249.

[6] A. Pandey, S. Kulkarni, A.P. Vincent, S.H. Nannuri, S.D. George, S. Mutalik, Hyaluronic acid-drug conjugate modified core-shell MOFs as pH responsive nanoplatform for multimodal therapy of glioblastoma, Int. J. Pharm. 588 (2020) 119735. https://doi.org/10.1016/j.ijpharm.2020.119735.

[7] H. Awala, S.M. Kunjir, A. Vicente, J.-P. Gilson, V. Valtchev, H. Seblani, R. Retoux, L. Lakiss, C. Fernandez, R. Bedard, S. Abdo, J. Bricker, S. Mintova, Crystallization pathway from a highly viscous colloidal suspension to ultra-small FAU zeolite nanocrystals, J. Mater. Chem. A. 9 (2021) 17492–17501. https://doi.org/10.1039/D1TA02781F.

[8] M. Zaarour, B. Dong, I. Naydenova, R. Retoux, S. Mintova, Progress in zeolite synthesis promotes advanced applications, Microporous Mesoporous Mater. 189 (2014) 11–21. https://doi.org/10.1016/j.micromeso.2013.08.014.

[9] V.J. Inglezakis, The concept of “capacity” in zeolite ion-exchange systems, J. Colloid Interface Sci. 281 (2005) 68–79. https://doi.org/10.1016/j.jcis.2004.08.082.

[10] O. Martinho, N. Vilaça, P.J.G. Castro, R. Amorim, A.M. Fonseca, F. Baltazar, R.M. Reis, I.C. Neves, In vitro and in vivo studies of temozolomide loading in zeolite structures as drug delivery systems for glioblastoma, RSC Adv. 5 (2015) 28219–28227. https://doi.org/10.1039/C5RA03871E.

[11] H. Awala, J.-P. Gilson, R. Retoux, P. Boullay, J.-M. Goupil, V. Valtchev, S. Mintova, Template-free nanosized faujasite-type zeolites, Nat. Mater. 14 (2015) 447–451. https://doi.org/10.1038/nmat4173.
[12] K. Goldyn, C. Anfray, S. Komaty, V. Ruaux, C. Hélaine, R. Retoux, S. Valable, V. Valtchev, S. Mintova, Copper exchanged FAU nanozeolite as non-toxic nitric oxide and carbon dioxide gas carrier, Microporous Mesoporous Mater. 280 (2019) 271–276. https://doi.org/10.1016/j.micromeso.2019.02.022.
[13] S. Komaty, H. Özçelik, M. Zaarour, A. Ferre, S. Valable, S. Mintova, Ruthenium tris(2,2'-bipyridyl) complex encapsulated in nanosized faujasite zeolite as intracellular localization tracer, J. Colloid Interface Sci. 581 (2021) 919–927. https://doi.org/10.1016/j.jcis.2020.08.117.
[14] W.-L.L. Suen, Y. Chau, Size-dependent internalisation of folate-decorated nanoparticles via the pathways of clathrin and caveolae-mediated endocytosis in ARPE-19 cells, J. Pharm. Pharmacol. 66 (2014) 564–573. https://doi.org/10.1111/jphp.12134.
[15] N. Vilaça, R. Totovao, E.A. Prasetyanto, V. Miranda-Gonçalves, F. Morais-Santos, R. Fernandes, F. Figueiredo, M. Bañobre-López, A.M. Fonseca, L.D. Cola, F. Baltazar, I.C. Neves, Internalization studies on zeolite nanoparticles using human cells, J. Mater. Chem. B. 6 (2018) 469–476. https://doi.org/10.1039/C7TB02534C.
[16] M.S. de Almeida, E. Susnik, B. Drasler, P. Taladriz-Blanco, A. Petri-Fink, B. Rothen-Rutishauser, Understanding nanoparticle endocytosis to improve targeting strategies in nanomedicine, Chem. Soc. Rev. 50 (2021) 5397–5434. https://doi.org/10.1039/D0CS01127D.
[17] A. Chakhoyan, J.-S. Guillamo, S. Collet, F. Kauffmann, N. Delcroix, E. Lechapt-Zalcman, J.-M. Constans, E. Petit, E.T. MacKenzie, L. Barré, M. Bernaudin, O. Touzani, S. Valable, FMISO-PET-derived brain oxygen tension maps: application to glioblastoma and less aggressive gliomas, Sci. Rep. 7 (2017) 10210. https://doi.org/10.1038/s41598-017-08646-y.
[18] Z. Liu, H. Tan, X. Zhang, F. Chen, Z. Zhou, X. Hu, S. Chang, P. Liu, H. Zhang, Enhancement of radiotherapy efficacy by silver nanoparticles in hypoxic glioma cells, Artif. Cells Nanomedicine Biotechnol. 46 (2018) S922–S930. https://doi.org/10.1080/21691401.2018.1518912.
[19] W.J. Brownlee, F.P. Seib, Impact of the hypoxic phenotype on the uptake and efflux of nanoparticles by human breast cancer cells, Sci. Rep. 8 (2018) 12318. https://doi.org/10.1038/s41598-018-30517-3.
[20] A. Musah-Eroje, S. Watson, Adaptive Changes of Glioblastoma Cells Following Exposure to Hypoxic (1% Oxygen) Tumour Microenvironment, Int. J. Mol. Sci. 20 (2019) 2091. https://doi.org/10.3390/ijms20092091.
[21] G.J. Doherty, H.T. McMahon, Mechanisms of endocytosis, Annu. Rev. Biochem. 78 (2009) 857–902. https://doi.org/10.1146/annurev.biochem.78.081307.110540.
[22] F. Lu, S.-H. Wu, Y. Hung, C.-Y. Mou, Size effect on cell uptake in well-suspended, uniform mesoporous silica nanoparticles, Small Weinh. Bergstr. Ger. 5 (2009) 1408–1413. https://doi.org/10.1002/smll.200900005.
[23] S. Paillas, R. Ladjohounlou, C. Lozza, A. Pichard, V. Boudousq, M. Jarlier, S. Sevestre, M. Le Blay, E. Deshayes, J. Sosabowski, T. Chardès, I. Navarro-Teulon, R.J. Mairs, J.-P. Pouget, Localized Irradiation of Cell Membrane by Auger Electrons Is Cytotoxic Through Oxidative Stress-Mediated Nontargeted Effects, Antioxid. Redox Signal. 25 (2016) 467–484. https://doi.org/10.1089/ars.2015.6309.
[24] J. Bourquin, D. Septiadi, D. Vanhecke, S. Balog, L. Steinmetz, M. Spuch-Calvar, P. Taladriz-Blanco, A. Petri-Fink, B. Rothen-Rutishauser, Reduction of Nanoparticle Load in Cells by Mitosis but Not Exocytosis, ACS Nano. 13 (2019) 7759–7770. https://doi.org/10.1021/acsnano.9b01604.
[25] T. Posati, F. Bellezza, L. Tarpani, S. Perni, L. Latterini, V. Marsili, A. Cipiciani, Selective internalization of ZnAl-HTlc nanoparticles in normal and tumor cells. A study of their potential use in cellular delivery, Appl. Clay Sci. 55 (2012) 62–69. https://doi.org/10.1016/j.clay.2011.10.006.

[26] N. Vilaça, A.R. Bertão, E.A. Prasetyanto, S. Granja, M. Costa, R. Fernandes, F. Figueiredo, A.M. Fonseca, L. De Cola, F. Baltazar, I.C. Neves, Surface functionalization of zeolite-based drug delivery systems enhances their antitumoral activity in vivo, Mater. Sci. Eng. C. 120 (2021) 111721. https://doi.org/10.1016/j.msec.2020.111721.
[27] L.H. Gray, A.D. Conger, M. Ebert, S. Hornsey, O.C.A. Scott, The Concentration of Oxygen Dissolved in Tissues at the Time of Irradiation as a Factor in Radiotherapy, Br. J. Radiol. 26 (1953) 638–648. https://doi.org/10.1259/0007-1285-26-312-638.
[28] M.R. Horsman, J. Overgaard, The impact of hypoxia and its modification of the outcome of radiotherapy, J. Radiat. Res. (Tokyo). 57 (2016) i90–i98. https://doi.org/10.1093/jrr/rrw007.
[29] J.J. Rennick, A.P.R. Johnston, R.G. Parton, Key principles and methods for studying the endocytosis of biological and nanoparticle therapeutics, Nat. Nanotechnol. 16 (2021) 266–276. https://doi.org/10.1038/s41565-021-00858-8.
[30] S. Vranic, N. Boggetto, V. Contremoulins, S. Mornet, N. Reinhardt, F. Marano, A. Baeza-Squiban, S. Boland, Deciphering the mechanisms of cellular uptake of engineered nanoparticles by accurate evaluation of internalization using imaging flow cytometry, Part. Fibre Toxicol. 10 (2013) 2. https://doi.org/10.1186/1743-8977-10-2.
[31] A.M. Bannunah, D. Vllasaliu, J. Lord, S. Stolnik, Mechanisms of Nanoparticle Internalization and Transport Across an Intestinal Epithelial Cell Model: Effect of Size and Surface Charge, Mol. Pharm. 11 (2014) 4363–4373. https://doi.org/10.1021/mp500439c.